Assessment of Cooling Rate in Longitudinal Welded Pipelines performed by Submerged Double-Arc Welding

E. Scutelnicu and C. C. Rusu

***Abstract*—** Combining the process parameters - from high pressure with low temperature to high temperature with no pressure - a wide range of welding processes by pressure and fusion have been developed in the last decades. Included in the group of fusion welding processes, submerged multi-arc welding is more and more applied to the pipelines manufacturing due to the increased productivity and efficiency of the process. In this case, an overlapping effect of temperature fields is manifested through a major influence on the cooling rate which is responsible for the metallurgical changes and, finally, for deterioration of the joints' mechanical characteristics. It is obvious that good performances of the welded joints ensure the quality and safety of metallic structures and a less impact on the environment is estimated to be achieved. That is why cooling rate should be theoretically and experimentally investigated. Moreover, distance between welding sources could be variable and leads to different values of cooling. The research focuses on the numerical modeling of heat transfer in the welded joints performed by submerged double-arc welding process distances between electric arcs is variable. Temperature field, thermal cycles and cooling rate versus different distances between thermal sources are comparatively analysed and discussed.

***Keywords*—**3D numerical model, pipelines, submerged double-arc welding, cooling rate.

I. Introduction

One of the most common pipeline materials is API-5L grade steel. The oil and gas industries have increased need for the use of High Strength Low Alloy (HSLA) steels such as API-5L-X70 and API-5L-X80, due to the cost savings they afford, especially in long piping systems that transport crude oil or natural gas. Microalloying with elements such as titanium, vanadium and niobium to produce these HSLA steel products are beneficial for the special features of theses steels which are very well related to the grain size nature. The nature and physical properties of precipitation are an important factor on the mechanical properties response characteristics of steels.

E. Scutelnicu is with the Department of Manufacturing Engineering, Faculty of Mechanical Engineering, "Dunarea de Jos" University of Galati, 800008 ROMANIA (corresponding author: +40336130212; fax: +40236461353; e-mail: elena.scutelnicu@ugal.ro).

C.C. Rusu is with the Department of Manufacturing Engineering, Faculty of Mechanical Engineering, "Dunarea de Jos" University of Galati, 800008 ROMANIA (e-mail: carmen.rusu@ugal.ro).

As *Sindo K.* reported [1], HSLA steels are designed to provide higher strengths than those of carbon steels, generally with minimum yield strengths of 275–550MPa. Besides manganese (up to about 1.5%) and silicon (up to about 0.7%), as in carbon steels, HSLA steels often contain very small amounts of niobium (up to about 0.05%), vanadium (up to about 0.1%), and titanium (up to about 0.07%) to ensure both grain refinement and precipitation hardening. As such, they are also called micro alloyed. Niobium (Nb), vanadium (V), and titanium (Ti) are strong carbide and nitride formers. Fine carbide or nitride particles of these metals tend to hinder the movement of grain boundaries, thus reducing the grain size by making grain growth more difficult. The reduction in grain size in HSLA steels increases their strength and toughness at the same time. This is interesting because usually toughness of steels decreases as their strength increases [1], [2].

The higher the heat input during welding, the more likely the carbide and nitride particles will dissolve and lose their effectiveness as grain growth inhibitors. The low toughness of the coarse-grain regions of the HAZ is undesirable. The HSLA steels are usually welded in the as-rolled or the normalized condition, and the weldability of most HSLA steels is similar to that of mild steel [1], [15]. The welding process strongly influences the performances of the metallic structures and their capacity to resist overload.

A greater attention should be given when HSLA steel is subjected to welding and then used for gas transport pipelines. The welding variables and the material properties affect the temperature profiles, cooling rates, microstructure and the resulting properties of the welded joint. Therefore, the welding effects should be minimized in order to preserve the special features of this steel grade, such as fine-grained achieved due to the presence of nitrides and/or carbides, finely distributed, high strength and high resistance to brittle cracking.

II. Cooling Rate

Taking into account the aspects described above, connected to the special features of HSLA steels, a great attention should be showed to the cooling rate and on the effects induced in the pipelines steel. Lee J. Y., Park J. M., Lee C. H. and Yoon E. P apud Sindo Kou measured the cooling rate and reported that increasing *EI/V*, the cooling rate decreases (Fig. 1) [3].

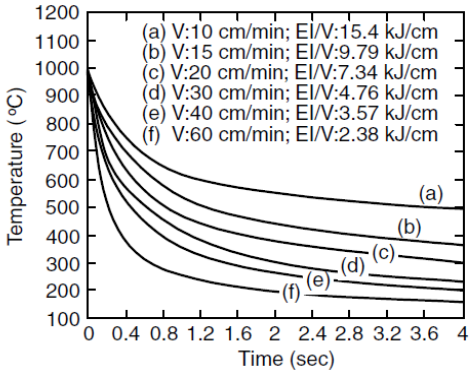

Fig. 1 Cooling rates vs. heat input per unit length of weld
Reprinted from Lee et. al. apud Sindo Kou [3]

Also, the heat generated during the welding process has a major influence on the cooling rate of the welded joint. For instance, the cooling rate in electroslag welding, which is known to have a very high *Q/V*, is much smaller than that in arc welding process and this phenomenon leads to different behaviour of the parent metal subjected to welding (Fig. 2) [4].

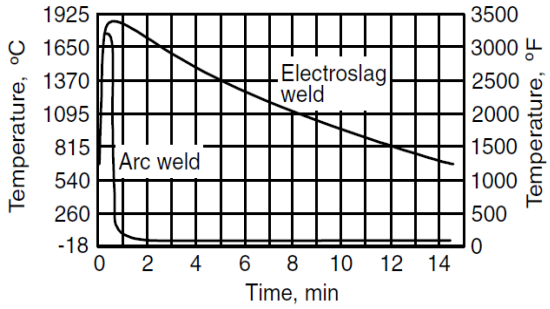

Fig. 2 Thermal cycles of electroslag and arc welds
Reprinted from Lee et. al. apud Sindo Kou [4]

Cooling rate, continuously, changes and for this reason specification of temperature range is absolutely necessary. For instance, a cooling rate of 10°C/s indicates a thermal cycle with low cooling at temperature of 1000°C, whereas at temperature of 200°C, the same value of cooling rate shows a thermal cycle with fast cooling in the transformation range. Frequently another parameter named $t_{8/5}$, representing the cooling time in the 800-500°C, range is preferred. A high cooling rate reflects a low value of $t_{8/5}$, influencing the peak temperature, hardness and extent of heat affected zone.

The upper limit of 800-500°C temperature range is placed below the GS line of Fe-C diagram, in order to take into account the shifting down of the austenite transformation. The lower limit of the temperature range corresponds to the minimum temperature at which the subcooling austenite has still stability. Below temperature of 500°C, austenite undergoes a transformation by diffusion called perlite transformation or without diffusion when non-equilibrium structures such as troostite, soorbite, bainite and martensite are achieved. For a specific chemical composition of base metal and a certain value of austenitizing parameter ($t_{8/5}$), the cooling time determines the nature of structural changes. Thus, the decrease of $t_{8/5}$ modifies the transformation mechanism by diffusion (pearlitic transformation) to the intermediate mechanism (bainitic transformation) or to that without diffusion (martensitic transformation).

When submerged double-arc welding (SDAW) procedure is applied, an overlapping effect of the temperature fields is developed and its influence on the cooling rate of the welded joint should be investigated. Moreover, distance between welding sources could be variable and leads to different values of cooling rate and, finally, to a deterioration of mechanical characteristics. In multiple-pass welding the interpass temperature is equivalent to the preheat temperature T_0 in single-pass welding. Preheating is a common practice in welding high-strength steels because it reduces the risk of heat-affected zone cracking. Besides, at higher welding speeds the cooling rate is higher and the cells are finer, while at lower welding speeds the cooling rate is lower and the cells are coarser.

A better understanding of the interdependence *temperature field - distance between welding sources - cooling rate* is compulsory, in order to determine the optimal distance so that the steel is not overheated and the grain coarsening is inhibited. Besides, the cooling rate of the joint has to be adequate so that a minimum impact on the special features of the base material should be achieved.

III. Model Description of SDAW

Nowadays, submerged multi-arc welding is more and more applied to the pipelines manufacturing due to the increased productivity and efficiency of the process in comparison with the classical submerged arc welding. Even in the classical variant, the transfer efficiency of energy from electrode source to work piece is very high (usually over 90%), since losses from radiation, convection, and spatter are minimal. Besides, the deposition rate is high and weld reliability is good [16].

In modeling of welding process, the heat source is often considered an ellipsoid model [5]. Goldak proposed a semi-ellipsoidal heat source and further improved into a double-ellipsoidal source in which the heat flux is distributed in a Gaussian manner throughout the volume of two semi-ellipsoids (Fig. 3) [6], [7]. The governing equation for transient heat transfer analysis is given by Eq. (1) and the spatial heat distribution, which is different in front and in the rear of the thermal source, can be computed by applying the equations (2) and (3) [5]-[7]:

$$\rho \cdot c \cdot \frac{\partial T}{\partial t}(x, y, z, t) = \nabla q(x, y, z, t) + Q(x, y, z, t) \quad (1)$$

$$q_f = \frac{6\sqrt{3} \cdot \eta \cdot Q \cdot f_f}{\pi\sqrt{\pi} \cdot a \cdot b \cdot c_f} \cdot e^{-3 \cdot \left(\frac{x^2}{a} + \frac{y^2}{b} + \frac{z^2}{c_f}\right)} \quad (2)$$

$$q_r = \frac{6\sqrt{3} \cdot \eta \cdot Q \cdot f_r}{\pi\sqrt{\pi} \cdot a \cdot b \cdot c_r} \cdot e^{-3 \cdot \left(\frac{x^2}{a} + \frac{y^2}{b} + \frac{z^2}{c_r}\right)} \quad (3)$$

where: *a, b* are ellipsoidal heat source dimensions;
c_f, c_r - source dimensions in front and rear of semi-ellipsoid;
f_f, f_r - coefficients of heat apportionment in front and in the rear of semi-ellipsoid $f_f + f_r = 2$;
q(x,y,z) - heat flux in a certain point *(x,y,z)*;
Q - heat input ($Q=\eta \cdot U \cdot I$);
U, I - welding voltage and amperage;
η - welding process efficiency.

Models based on a double-ellipsoidal heat source used to simulate the butt SDAW were developed in many references [9], [11], [13]. Two ellipsoid models, having different dimensions, have been considered to the development of the present complex model. The schematic view of heat sources with the axis system, illustrated in Fig. 4, shows their position on the sheets of pipeline steel. The dimensions of the thermal sources are indicated below.

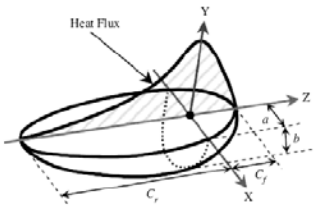

Fig. 3 Goldak'model of thermal source

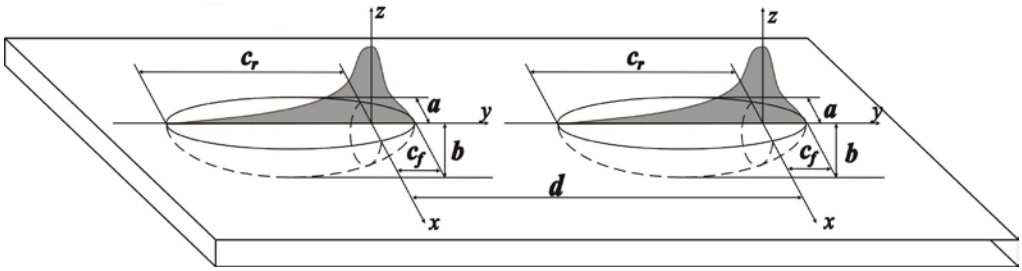

Fig. 4 Schematic view of heat sources location

The investigation focussed on the submerged arc welding in two separated welding pools, as Tandem - Submerged Arc Welding (SAW) variant works (Fig. 5). Because of the model symmetry and to gain computing time, the modeling and simulation of process have been made on half model of joint.

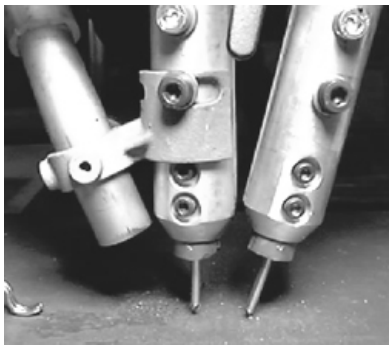

Fig. 5 Tandem SAW variant

The heat transfer in the joint of two API-5L-X70 steel plates with similar dimensions (500 mm × 300 mm × 19.1 mm), was modelled as 3D heat transfer problem. Taking into account the real dimensions of sheets, a complex numerical model has been developed by the authors. A mesh refining of the welding pool and heat affected zone (HAZ) was made in order to achieve better numerical results.

It is well known that the accuracy of the numerical results is strongly connected to the accuracy of the data input. The numerical model has been developed, taking into consideration the following assumptions:

- isotropy of the base material
- thermo-physical properties versus temperature
- heat flux losses by convection and radiation.

The initial temperature of the base metal introduced in the model was 20°C. The welding speed and heat input are considered constant during the whole process, whilst the welding source moves continuously - heating and melting new regions in front of it - and keeps its influence on the weld pool, as too. Two time functions - corresponding to each heat source positioned on the plates - have been developed as a succession of triangle functions in order to simulate their movement along the longitudinal axis of the joint. The temperature field is the result of the total thermal effects during the welding process starting from the initial moment of the process, t=0, until the final moment, $t=t_n$ [14. According to the notations from Fig. 4, data related to *a, b*, c_f, c_r specific to the SDAW, which were introduced in the numerical model, are the following:

- First source: a=6,5mm b=7mm, c_f=7mm, c_r=20mm;
- Second source: a=5mm b=7mm, c_f=7mm, c_r=19mm.

IV. Results and Discussions

At the beginning of the process, due to the low temperature of the plates and the instability of the process, heat affected zone (HAZ) is less extended. In the steady-state or equilibrium phase, the welding process is stabilized and the temperature field has the same shape and extent in each moment. In the areas where the influence of the heat sources is strongest, the temperature gradients are high, involving a specific behaviour of the base material and a degradation of its mechanical and metallurgical properties.

The captures of the temperature field both in the transient phase and steady-state, at different moments of the welding process, are presented in Fig. 6 to 8. The peak temperatures reached within the heating phases is strongly dependent on the distance between the welding sources. Besides, due to the increase of distance, time needed to reach the peak temperatures increases with increase of distance. For instance, when the distance between the welding sources is 50 mm (Fig. 6), the peak temperature is 2088ºC and is reached after 34s from the beginning of the welding process. Similarly, when the distance is 100mm, the peak temperature is 1965ºC recorded after 42s (Fig. 7) and 1922ºC reached after 50s when the distance is 150 mm (Fig. 8).

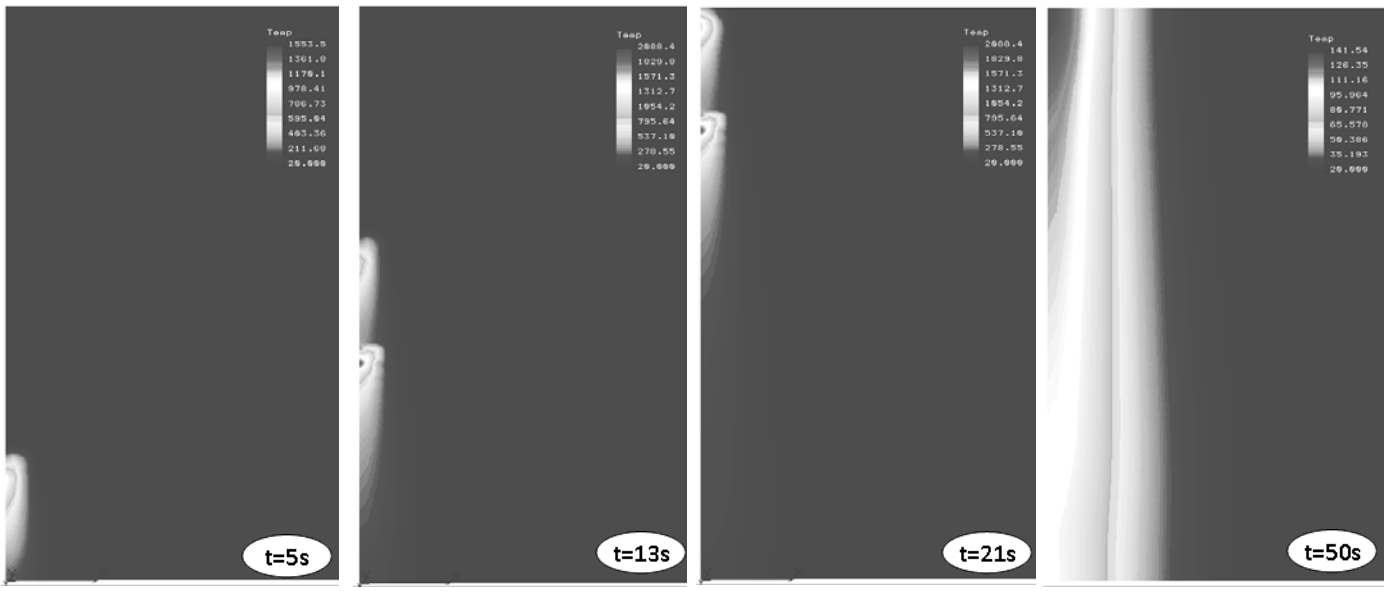

Fig. 6 Temperature field when distance between welding sources is 50 mm

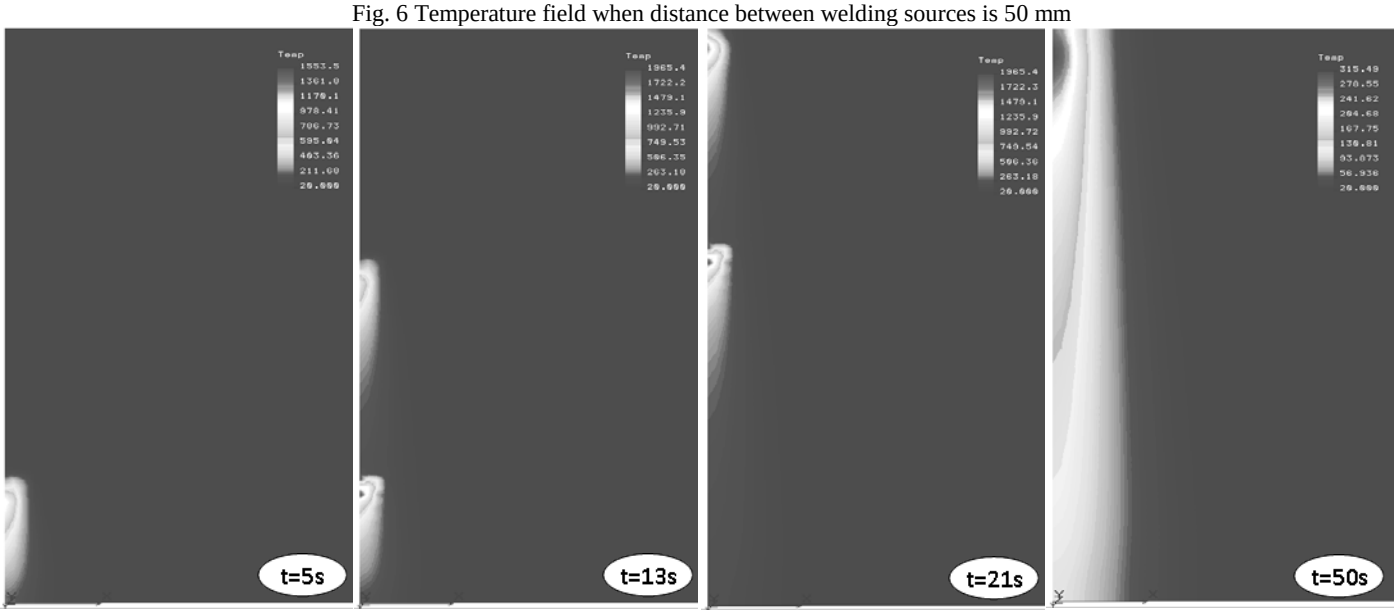

Fig. 7 Temperature field when distance between welding sources is 100 mm

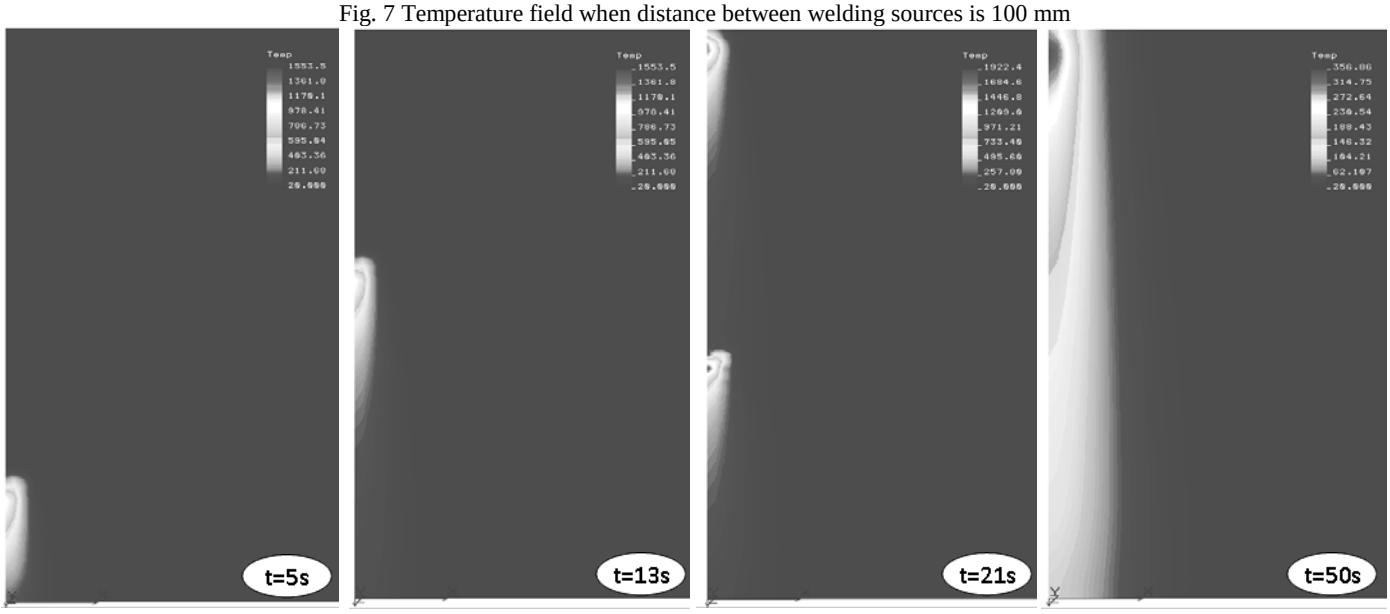

Fig. 8 Temperature field when distance between welding sources is 150 mm

It is interesting to notice that the peak temperature is achieved in the area of the second temperature, first heat source playing a preheating role of the sheets. The second welding source moves behind the first thermal source and fills the gap between the plates.

The modeling outputs were processed and charts of thermal history - representing temperature vs. time - in four nodes (x=0mm, x=17mm, x=15mm, x=19,1mm) located at different depths from the top of sheet were plotted (Fig. 9). A specific double shape of thermal cycles (heating-cooling-heating-cooling) is achieved in the case of SDAW. When the first heat source approaches the nodes, the temperature rises very rapidly and reaches the maximum value when welding source is closest to them. The temperature remains at that maximum as long as the source remains close to that point, in the welding case is only an instant, as the heat source continuously moves. Then, first source moves away and first cooling phase begins and lasts few seconds. After that, due to the approaching of the second heat source, the temperature increases again and decreases for the second time at a rate dependent on the thermal mass and thermal-physical properties of the material.

The maximum temperature is up to 14 to 18% respectively higher in comparison with peak temperature of first thermal cycle, but inversely proportional with the increase of distance between electric arcs. The increase of the distance between welding sources leads to increase of time before the beginning of the second heating phase. That phenomenon has an important influence on the structure modifications and compounds which could occur in the fusion zone and HAZ.

The maximum maximorum value of temperature is 2088ºC, corresponding to distance between heat sources of 50mm, well above the liquidus temperature of steel. It is important to ensure that melting is complete and right fluidity is achieved in order to allow parent and filler materials to flow properly into the weld groove. If distance increases, the peak temperature recorded in the centre of the second welding is slightly decreasing with 2-3%, as Fig. 9 illustrates.

In the heat-affected zone, the base metal does not undergo melting. However, in individual areas of this region the effects of heating and cooling can change the properties and structure of the base metal in various ways. That is why cooling rate is important in achievement of safe joints and should be investigated.

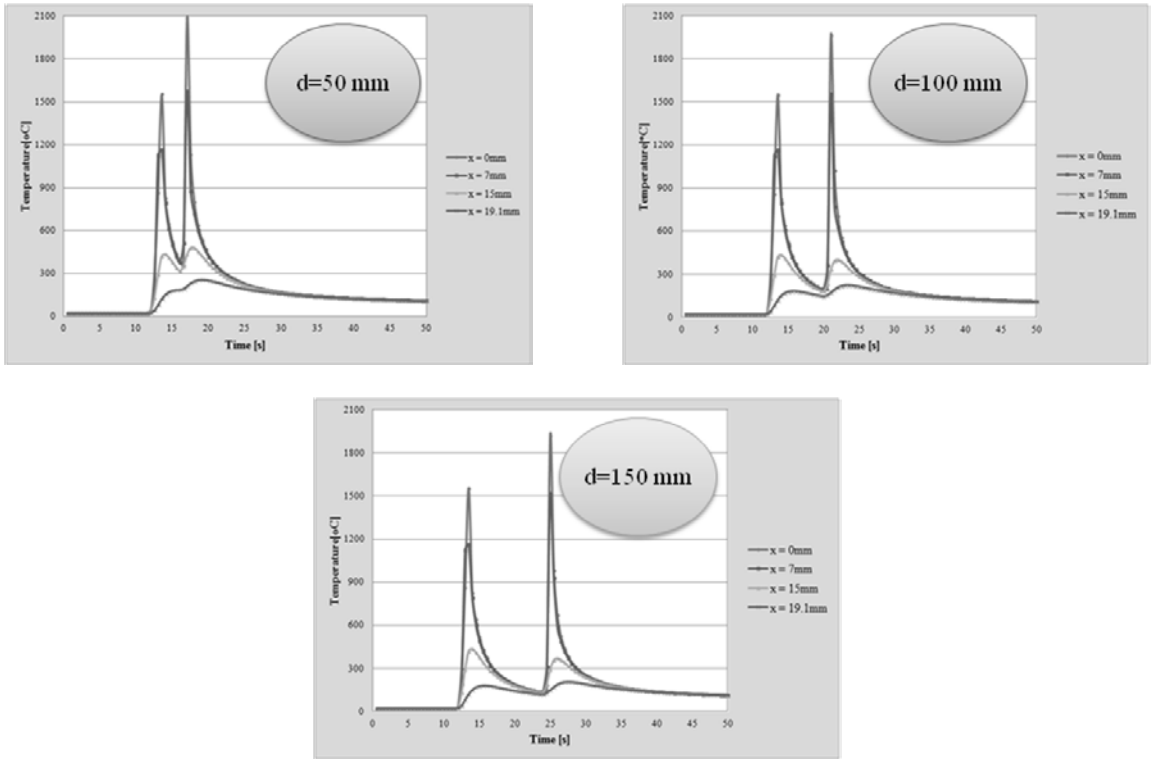

Fig. 9 Thermal history of weld depending on the distance between welding sources

Numerical data related to heating/cooling rates were processed and plotted (Fig. 10). They are correlated with the complex cycle developed during the SDAW process. Because the thermal cycles are different, it is expected that the heating/cooling rates are different, too. The heating/cooling rate was computed as difference between temperatures values reported to an interval of one second. The results are conclusive and show the major influence of distance on the heating/cooling rate. It can be noticed that the highest cooling rate is achieved when the distance is smallest and decreases with distance increasing. Changing the distance between thermal sources, the distribution of temperature is changed, but also cooling speed of joint. That means a different mechanical and metallurgical behaviour of parent metal subjected to welding, with implications on the safety of pipelines used for gas transport. However, achievement of optimal mechanical properties of the welded joint should remain the most important quality criteria.

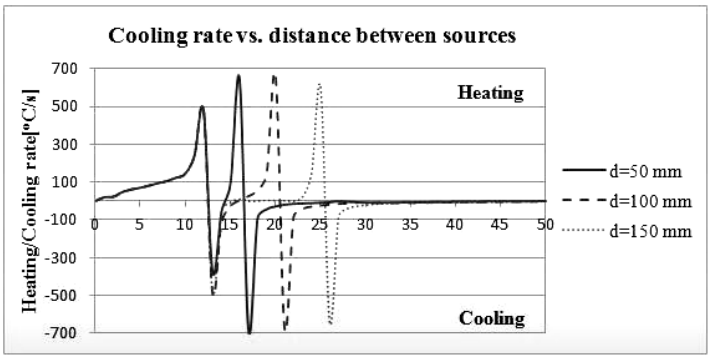

Fig. 10 Thermal history of weld depending on the distance between welding sources

V. Conclusion

Three dimensional finite element model of longitudinal butt welded joint performed by SDAW was developed and described in this paper. There are several specific aspects that have to be emphasised when the distance between the welding sources is variable:

- A specific heating-cooling-heating-cooling complex cycle is developed during SDAW.
- Distance between welding sources has a great influence on thermal history determined by the process and on heating/cooling rates registered during the specific thermal cycles.
- Due to the increase of distance, time needed to reach the peak temperatures increases with increase of distance.
- Changing the distance between thermal sources, the distribution of temperature and cooling speed of joint are changed and mechanical and metallurgical behaviour of parent material are influenced.
- The highest cooling rate is achieved when the distance is smallest and decreases with distance increasing.

In order to have a complete view on the pipeline steel behaviour, an investigation of mechanical and metallurgical changes, so that the optimum distance, corresponding to the achievement of best properties of the base material, should be made and correlated with data achieved on temperature field, thermal cycles and cooling rate described in this work.

Acknowledgment

This work was supported by the Romanian National Authority for Scientific Research, CNDI– UEFISCDI, through grant 27/2012, project number PN-II-PT-PCCA-2011-3.1-1057.

References

[1] M. Abid, M. J. Qarni, "3D thermal finite element analysis of single pass girth welded low carbon steel pipe-flange joints", *Turkish J. Eng. Env. Sci.* 33 (2009), doi: 10.3906/muh-0912-6, pp. 281–293 apud Goldak J., Chakravarti A., Bibby M., "A new finite element model for welding heat source", *Metallurgical Transactions B* 15B, 1984, pp. 299–305.

[2] D. C. Birsan, C. C. Rusu, E. Scutelnicu, Mistodie L. R., "Heat transfer analysis in API X70 steel joints performed by double submerged arc welding process", *Metalurgia International*, ISSN 1582-2214, Vol. XVIII/1, 2013, pp. 62-65.

[3] J. Goldak, M. Bibby, J. Moore, R. House, B. Patel, "Computer modeling of heat flow in welds", *Metallurgical Transactions B*, vol. 17 B, 1986, pp. 587-600.

[4] F. Kong, J. Ma, R. Kovacevic, "Numerical and experimental study of thermally induced residual stress in the hybrid laser–GMA welding process", *Journal of Materials Processing Technology* 211 (2011) 1102–1111 apud J. Goldak, A. Chakravarti, M. Bibby, "A new finite element model for welding heat source", *Metallurgical Transactions* B 15B, 1984, 299–305.

[5] J. Y. Lee, J. M. Park, C. H. Lee, E. P. Yoon, *Synthesis/Processing of Lightweight Metallic Materials II*, Eds. C. M. Ward-Close, F. H. Froes, S. S. Cho and D. J. Chellman, The Minerals, Metals and Materials Society, Warrendale, PA, 1996, p. 49. apud Sindo, Kou, *Welding Metallurgy*, John Wiley & Sons, Inc., Hoboken, New Jersey, USA, 2003, p. 55

[6] E. Leonard Samuels, *Light Microscopy of Carbon Steels*, ASM International, USA, 1999, p.82.

[7] S. Liu, S. D. Brandi, R. D. Thomas, *ASM Handbook*, Vol. 6, ASM International, Materials Park, OH, 1993, p. 270 apud Sindo, Kou, *Welding Metallurgy*, John Wiley & Sons, Inc., Hoboken, New Jersey, USA, 2003, p. 56

[8] K. Sindo, *Welding Metallurgy*, University of Wisconsin, 1987.

[9] E. Scutelnicu, C. C. Rusu, E. Constantin, V. Teodor, "Prediction of Cooling Rate in API-5L-X70 Steel Plates welded by Submerged Double-Arc Welding", *Proceedings of 1st WSEAS International Conference on Industrial and Manufacturing Technologies - INMAT'13*, 14-16 Mai 2013, Vouliagmeni, Greece, pp. 52-57.

[10] L. R. Mistodie, E. Constantin, C. Voicu, V. Teodor, "Experimental Research on Submerged Multi-arc Welding of API-5L-X70 Steel", *Proceedings of 1st WSEAS International Conference on Industrial and Manufacturing Technologies - INMAT'13*, 14-16 Mai 2013, Vouliagmeni, Greece, pp. 227-232.

[11] C.C. Rusu, E. Scutelnicu, L. R. Mistodie, V. Teodor, "Numerical Models for Simulation of Submerged Double Arc Welding Process", *Proceedings of 1st WSEAS International Conference on Industrial and Manufacturing Technologies - INMAT'13*, 14-16 Mai 2013, Vouliagmeni, Greece pp. 233-238.

[12] A. Moarrefzadeh, M. A. Sadeghi, *Numerical Simulation of Thermal Profile By Gas Tungsten Arc Welding Process in Copper*, *WSEAS TRANSACTIONS on HEAT and MASS TRANSFER*, Issue 3, Volume 5, July 2010, pp. 53-62.

[13] E. Scutelnicu, M. Iordachescu, M. Blasco, D. Iordachescu, "Arc Welding of Dissimilar Metals: FEA and Experiments", *Proceedings of 8th International Conference on Trends in Welding Research*, June 2-6 2008, Pine Mountain, Georgia USA, ASM International, pp. 241-246.

[14] E. Constantin, E. Scutelnicu, C. C. Rusu, L. Mistodie, C. Voicu, D. Boazu, "FEA and experiments in case of pipelines welding", *Proceedings of the 2nd South East European IIW International Congress, Welding – HIGH-TECH Technology in 21st century, Pipeline Welding Current Topic of the Region*, Bulgaria, 2010, pp. 254-257.

[15] ****Corrosion of Weldments*, ASM International, Edited by J. R. Davis, Davis & Associates, USA, 2006.

[16] http://libback.uqu.edu.sa/hipres/Indu/indu10740.pdf